T Cell-to-Stroma Enrichment (TSE) score: a gene expression metric that predicts response to immune checkpoint inhibitors in patients with urothelial cancer

Maud Rijnders[1,*], J. Alberto Nakauma-González[1,2,3,*], Debbie G.J. Robbrecht[1], Alberto Gil-Jimenez[4,5], Maureen J.B. Aarts[6], Joost L. Boormans[2], Paul Hamberg[7], Michiel S. van der Heijden[4,8], Bernadett E. Szabados[9], Geert J.L.H. van Leenders[10], Niven Mehra[11], Jens Voortman[12], Hans M. Westgeest[13], Ronald de Wit[1], Astrid A.M. van der Veldt[1,14], Reno Debets[1,*], Martijn P. Lolkema[1,*]

[1]*Departments of Medical Oncology, Erasmus MC Cancer Institute, University Medical Center Rotterdam, Rotterdam, the Netherlands*
[2]*Department of Urology, Erasmus MC Cancer Institute, University Medical Center Rotterdam, Rotterdam, the Netherlands*
[3]*Cancer Computational Biology Center, Erasmus MC Cancer Institute, University Medical Center Rotterdam, Rotterdam, the Netherlands*
[4]*Department of Molecular Carcinogenesis, the Netherlands Cancer Institute, Amsterdam, the Netherlands*
[5]*Oncode Institute, Utrecht, the Netherlands*
[6]*Department of Medical Oncology,* GROW-School for Oncology and Reproduction*, Maastricht University Medical Center, Maastricht, the Netherlands*
[7]*Department of Medical Oncology, Franciscus Gasthuis & Vlietland Hospital, Rotterdam/Schiedam, the Netherlands*
[8]*Department of Medical Oncology, the Netherlands Cancer Institute, Amsterdam, the Netherlands*
[9]*Barts Cancer Institute, Queen Mary University of London, London, UK*
[10]*Department of Pathology, Erasmus MC Cancer Institute, University Medical Center Rotterdam, Rotterdam, the Netherlands*
[11]*Department of Medical Oncology, Radboud University Medical Center, Nijmegen, the Netherlands*
[12]*Department of Medical Oncology, Amsterdam UMC, Vrije Universiteit Amsterdam, Cancer Center Amsterdam, Amsterdam, the Netherlands*
[13]*Department of Internal Medicine, Amphia Hospital Breda, Breda, the Netherlands*
[14]*Radiology & Nuclear Medicine, Erasmus MC Cancer Institute, University Medical Center Rotterdam, Rotterdam, the Netherlands*
* Contributed equally

Corresponding author

Dr. Martijn P. Lolkema

Dr. Molewaterplein 40, 3015 GD Rotterdam, The Netherlands

Email: m.lolkema@erasmusmc.nl

Direct dial: +31 10 704 19 06

Abstract

Immune checkpoint inhibitors (ICIs) improve overall survival in patients with metastatic urothelial cancer (mUC). To identify predictive markers of response, whole-genome DNA (n=70) and RNA-sequencing (n=41) were performed using fresh metastatic biopsies prior to treatment with pembrolizumab. PD-L1 combined positivity score failed, while tumor mutational burden and APOBEC mutagenesis modestly predicted response. Using gene expression analysis, we defined the T cell-to-stroma enrichment (TSE) score, a signature-based metric that captures the relative abundance of T cells and stromal cells. Patients with a positive and negative TSE score show progression free survival rate at 6 months of 67% and 0%, respectively. The significant predictive value of the TSE score was validated in two independent ICI treated cohorts of patients with mUC (IMvigor210) and muscle-invasive UC (ABACUS). The TSE score represents a clinically applicable marker that may select patients with metastatic and primary UC who do not benefit from ICI treatment.

57 **Introduction**

58 Immune checkpoint inhibitors (ICIs) directed against programmed cell death protein
59 (PD-1) or its ligand (PD-L1) have significantly improved clinical outcomes of patients
60 with metastatic urothelial cancer (mUC). In patients with mUC with progressive disease
61 after platinum-based chemotherapy, treatment with pembrolizumab (anti-PD-1)
62 showed superior survival outcomes as compared to second-line chemotherapy in a
63 phase 3 trial[1,2]. A small subset of these patients had a durable response for years[3].
64 Furthermore, first-line treatment with pembrolizumab and atezolizumab (anti-PD-L1)
65 showed efficacy in single-arm trials[4,5]. Several clinical trials are currently investigating
66 the efficacy of ICIs for patients with muscle-invasive bladder cancer (MIBC)[6]. Notably,
67 the overall response rate is still limited in patients with mUC having the disadvantage
68 of exposing all patients to potential (severe) toxicities and expensive therapies.

69 To date, the only biomarker available to select patients with mUC for ICIs is PD-L1
70 protein staining in tumor tissue. However, the predictive value of PD-L1 expression
71 heavily depends on the population of patients studied[1,4,5,7-9]. Furthermore, an important
72 limitation of evaluation of PD-L1 protein expression is its dependence on a specific
73 staining platform, and use of archival tumor tissue[10,11].

74 Another biomarker that is associated with response to ICIs is tumor mutational burden
75 (TMB)[12,13]. Recently, high TMB (≥10 mutations per mega base-pair) was approved by
76 the U.S. Food and Drug Administration as a pan-cancer metric to select patients with
77 previously treated advanced solid tumors for treatment with pembrolizumab[14,15].
78 Furthermore, immune cell infiltration[16-18], expression of immune genes such as *IFNG,*
79 *CXCL9 and CXCL10*[16,19], TGF-β signaling[20], composition of the tumor
80 microenvironment[21], alterations in DNA damage repair (DDR) genes[22], abundance of
81 circulating tumor DNA[23,24] and the diversity of the T cell receptor (TCR) repertoire[16,25,26]

82 have all been associated with response and resistance to ICIs. Other studies suggest
83 that the combination of multiple biomarkers improves response prediction for patients
84 with mUC when compared to single biomarkers[27,28]. Collectively, there is still a lack of
85 evidence and validation of above-mentioned biomarkers in patients with mUC.

86 Along this line, we have performed whole-genome DNA-sequencing (WGS) and RNA-
87 sequencing (RNA-seq) and applied an integrative approach towards the discovery of
88 new predictors for response to ICIs in patients with mUC. We identified the T cell-to-
89 stroma enrichment (TSE) score, a transcriptomic measure comparing the expression
90 scores of T cell and stromal cell related gene expression signatures as a robust and
91 easy to implement metric to predict response to anti-PD-1 in mUC. The predictive value
92 of this score was confirmed in two independent cohorts of patients with primary and
93 metastatic UC treated with anti-PD-L1.

94

Results

Patient cohort and clinical characteristics

Between March 1st 2013 and March 31st 2020, 288 patients with advanced or mUC were included in the Center for Personalized Cancer Treatment (CPCT-02) biopsy protocol (NCT01855477; **Fig. 1**). Fresh-frozen metastatic tumor biopsies and matched normal blood samples were collected for WGS and RNA-seq as described previously[29]. Seventy patients received pembrolizumab monotherapy and were included in this analysis. Matched RNA-seq was available for 41 patients. PD-L1 combined positivity score (CPS) was assessed in biopsies of 40 patients.

One-third (n = 24) of patients who received pembrolizumab were responders according to response evaluation criteria in solid tumors (RECIST) v1.1. The PD-L1 CPS was positive (≥10) in 21% of responders and 24% of non-responders. Most patients (90%) received pembrolizumab as second-line therapy, but responders more frequently received pembrolizumab as first-line therapy compared to non-responders (25% *vs* 2%; Fisher's exact test p = 0.005; chemotherapy-naïve patients were selected for a positive PD-L1 CPS). At data cut-off, 27% of patients were alive. The median overall survival (OS) was 8.9 months, and the median progression-free survival (PFS) was 2.9 months. Patient characteristics are summarized in **Supplementary Table 1**.

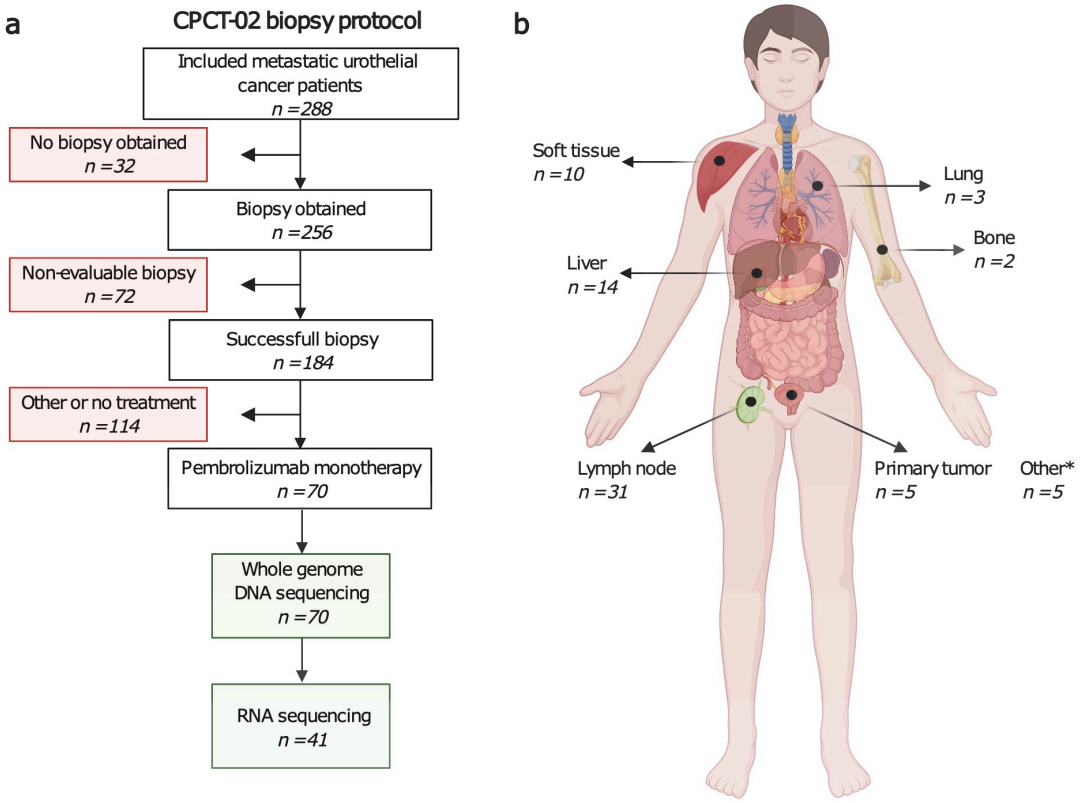

Fig. 1: Study design and biopsy sites of patients with metastatic urothelial cancer treated with pembrolizumab.

(a) Flowchart of patient inclusion. Patients with advanced or metastatic urothelial cancer who were scheduled for systemic palliative treatment were selected from the prospective Center for Personalized Cancer Treatment (CPCT-02) patient cohort (n = 288). Patients were excluded if no tumor biopsy was obtained, the biopsy was non-evaluable (tumor cell percentage <20%), or in case patients were not treated with pembrolizumab monotherapy after biopsy. As a result, 70 patients were included for analysis. Whole-genome DNA sequencing (WGS) data were available for all 70 patients. Matched RNA-sequencing data were available for 41 of these patients. (**b)** Overview of the number of biopsies per metastatic site included in this study. Primary tumor samples were obtained from patients with locally advanced disease with synchronous distant metastases that were not safely accessible for a biopsy. *Other biopsy sites included adrenal gland (n = 2), peritoneum (n = 2), and local recurrence of the primary tumor (n = 1). Created with BioRender.com.

129

130 **TMB and APOBEC mutagenesis only modestly predict response to**
131 **pembrolizumab**

132 The majority of patients (54%) in our cohort had a high TMB (**Fig. 2)**. Of patients with
133 high TMB, 47% were responders, whereas only 19% of patients with low TMB were
134 responders (Fisher's exact test p = 0.022; **Supplementary Fig. 1**). Previously, five
135 genomic subtypes (GenS) of mUC were identified according to COSMIC v3.1
136 mutational signatures[30]. GenS1, which is related to APOBEC mutagenesis, was
137 identified in 61% of samples. Overall, genomic subtypes were not associated with
138 treatment response. Of patients with high APOBEC mutagenesis (n = 29), 48%
139 responded to pembrolizumab, whereas 24% of patients with non-high APOBEC
140 mutagenesis (n = 41) responded to pembrolizumab (Fisher's exact test p = 0.045;
141 **Supplementary Fig. 1**). One responder had no evidence of APOBEC mutagenesis
142 but had a high TMB as a result of defective DNA mismatch repair. We did not observe
143 differences between responders and non-responders with respect to HR deficiency nor
144 presence of chromothripsis.

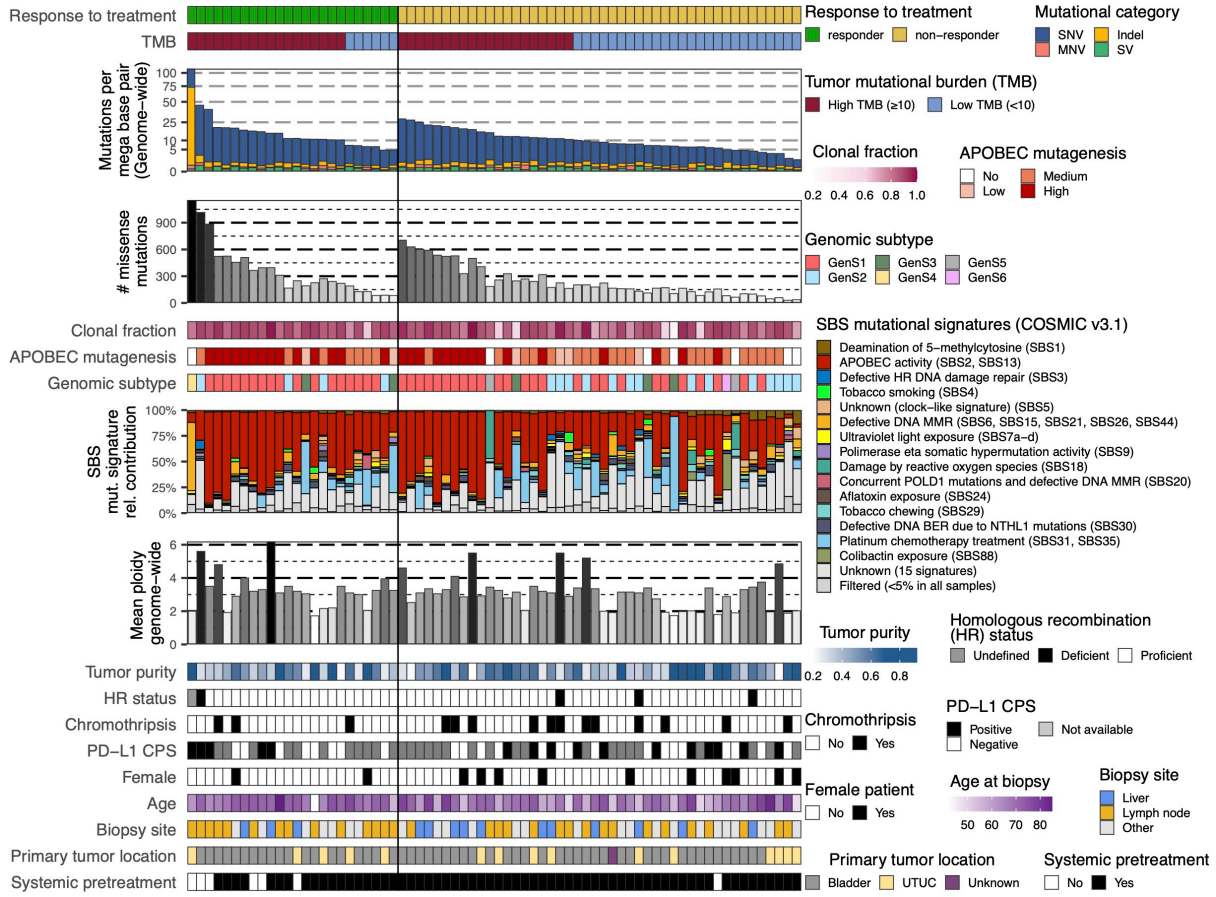

Fig. 2: The genomic landscape of patients with metastatic urothelial carcinoma treated with pembrolizumab.

Whole-genome sequencing data from biopsy samples of patients with metastatic urothelial carcinoma (n = 70) are displayed according to treatment response at 6 months of therapy (responder: ongoing complete or partial response, or stable disease, n = 24; non-responder: progressive disease, n = 46). Genomic and clinical features are listed from top to bottom as follows: genome-wide tumor mutational burden (TMB), and classification into high and low; total number of missense mutations; clonal fraction of mutations; APOBEC enrichment analysis showing tumors with no-, low-, medium- and high-APOBEC mutagenesis; genomic subtypes according to mutational signatures[30]; single base substitution (SBS) mutational signatures according to COSMIC v3.1; genome-wide mean ploidy; tumor purity; homologous recombination (HR) status; tumors with at least one chromothripsis event; PD-L1 combined positivity score (CPS) according to the companion diagnostic assay of pembrolizumab

159 (positive: CPS ≥ 10, negative: CPS < 10, or not available (NA)); female patients; age at time
160 of biopsy; metastatic site from which a biopsy was obtained; primary tumor location (bladder
161 or upper tract urothelial carcinoma, UTUC); and patients who received systemic treatment prior
162 to start of anti-PD-1 therapy.
163

164 Furthermore, when evaluating driver gene alterations, we did not observe statistically
165 significant differences between responders and non-responders (**Supplementary Fig.**
166 **2**). Alterations in canonical signaling pathways were most frequently observed in the
167 p53, cell cycle, and RTK-RAS pathways (**Supplementary Fig. 3a**), yet not significant
168 difference between the two patient groups. Also, the frequency of alterations in DDR
169 genes and signaling pathways was not statistically different between responders and
170 non-responders (**Supplementary Fig. 3b**). Activity of the p53 pathway was reduced in
171 those patients (responders and non-responders alike) with genomic alterations in this
172 pathway (**Supplementary Fig. 3c**). Collectively, the genomic analyses revealed only
173 modest predictive value of TMB and APOBEC mutagenesis for response to anti-PD-1.
174

175 **Expression of genes representing immune cells and stromal cells distinguishes**
176 **responders from non-responders to pembrolizumab**

177 Differential gene expression analysis of matched RNA-seq data (n = 41) revealed that
178 up-regulated genes in responders *vs* non-responders were part of the chemokine
179 pathway, and a pathway related to interactions between lymphoid and non-lymphoid
180 cells (**Fig. 3**). Down-regulated genes in responders (up-regulated in non-responders)
181 were related to extracellular matrix organization and collagen formation, generally
182 linked to the activity of stromal cells.

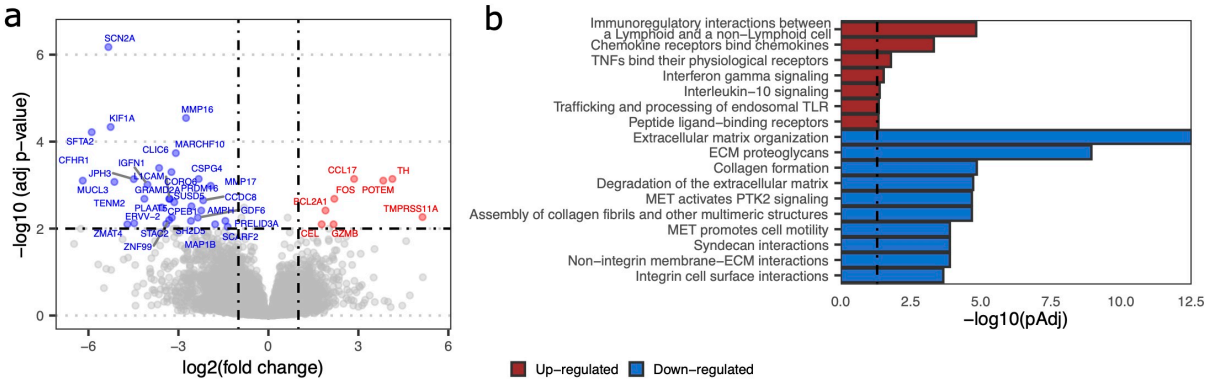

Fig. 3: Differential expression of genes and pathways related to immune cell and stromal cell activity for responders and non-responders to pembrolizumab.

(a) Volcano plot showing genes with up-regulated or down-regulated expression in responders (n = 13) *vs* non-responders (n = 28). Genes of which differential expression analysis showed adjusted p-value < 0.01 and absolute log2 fold change >1 are labelled in red (up-regulated) and blue (down-regulated). (**b)** Bar diagram specify the pathways of differentially expressed genes (adjusted p-value < 0.1 and absolute log2 fold change >1) according to ReactomePA v1.34.0[31]. Enriched pathways with adjusted p-value < 0.05, indicated by the vertical dashed line, were considered significant. All significantly up-regulated pathways, and the top ten down-regulated pathways are displayed.

Patient stratification according to T cell-to-stroma enrichment score coincides with response to pembrolizumab

Following up on the pathway analysis displayed in **Fig. 3**, we interrogated the transcriptomic landscape of our cohort for expression of a broad list of gene signatures related to T cells, other (non-T cell) immune cells, and stromal cells and their products (see **Supplementary Table 2** for a detailed overview of all gene signatures). Some of these signatures have been reported as predictors of response and resistance to ICIs[18,20]. Hierarchical clustering according to all the signatures revealed three distinct patient clusters (**Fig. 4**). In cluster one (n = 18), 61% of patients showed a response to

204 pembrolizumab. These patients predominantly had high signature scores for T cells
205 and other immune cells. In cluster two (n = 10), 20% of patients showed a response to
206 pembrolizumab. These patients generally had a similar score for all signatures. In
207 cluster three (n = 13), none of the patients showed a response to pembrolizumab.
208 These patients predominantly had high signature scores for stromal cells and their
209 products. The above clustering suggested that signature expression scores for
210 immune cells and stromal cells and their products were related to response to
211 pembrolizumab. To select those signatures with the most predictive value, ROC curves
212 were constructed per signature, which demonstrated areas under the curve (AUC) that
213 ranged from 0.54 to 0.77 (median = 0.68; **Supplementary Table 3**). The highest AUCs
214 (> 0.7) were observed for T cells and stromal cells and their products, and all (non-T
215 cell) immune cells had an AUC below the median. Sets of signatures that showed the
216 highest AUCs and highest discriminatory power were selected and combined into a
217 global T cell and a global stromal signature (**Supplementary Fig. 4**). Notably, logistic
218 regression analyses showed that the global T cell signature was an independent
219 predictor of response (Coefficient = 3.03, p = 0.005), while the global stromal signature
220 was an independent predictor of non-response (Coefficient = -2.40, p = 0.010) to
221 pembrolizumab. Next, we combined these two global signatures into a single metric
222 that we termed the T cell-to-stroma enrichment (TSE) score that reflects the
223 abundance of T cells relative to that of stromal cells and their products. This TSE score
224 revealed a significantly higher predictive value (AUC = 0.88) for treatment response
225 than either global or individual signatures alone (**Supplementary Table 3**). Stratifying
226 patients by their TSE score resembled the patient groups obtained by hierarchical
227 clustering and revealed almost identical response rates (67%, 21% and 0% for patients
228 with a positive, neutral or negative TSE score).

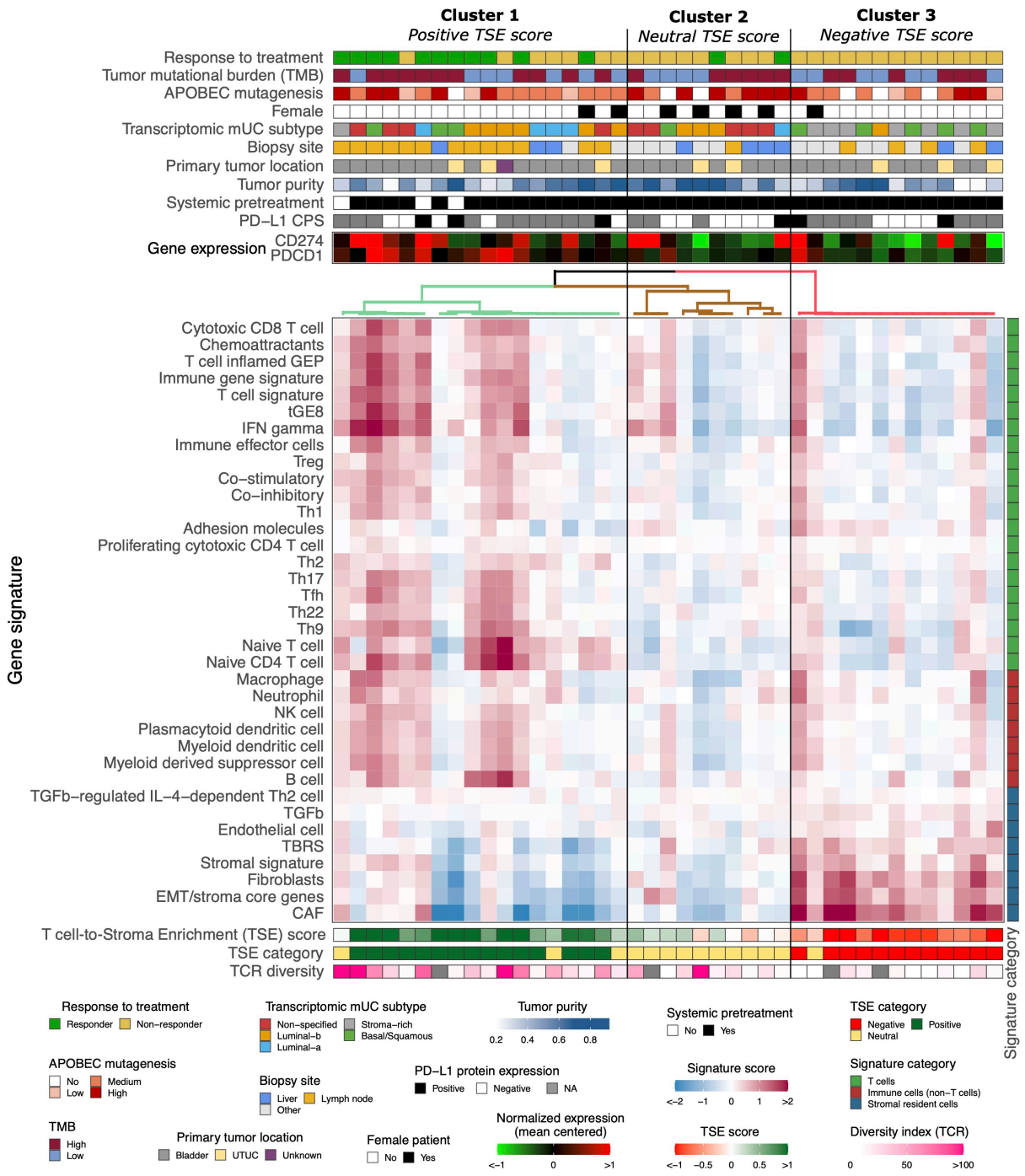

Fig. 4: Hierarchical clustering of gene signatures representing T cells, immune cells and stromal cells and their products distinguishes responders from non-responders to pembrolizumab.

Transcriptomic profile of 41 out of 70 patients with metastatic urothelial carcinoma (mUC), clustered using ConsensusClusterPlus v1.54.0[32] according to gene signature scores. Transcriptomic and clinical features are listed from top to bottom as follows: response to

236 treatment at 6 months of therapy (responder: ongoing complete or partial response, or stable
237 disease, n = 13; non-responder: progressive disease, n = 28); tumor mutational burden (TMB);
238 APOBEC enrichment analysis showing tumors with no-, low-, medium- and high-APOBEC
239 mutagenesis; transcriptomic subtypes of mUC[30]; biopsy site; primary tumor location (bladder
240 or upper tract urothelial carcinoma, UTUC); tumor purity; patients who received systemic
241 treatment prior to start of anti-PD-1 therapy; PD-L1 combined positivity score (CPS; positive:
242 CPS ≥ 10, negative: CPS < 10, or not available (NA)); *CD274* (PD-L1) and *PDCD1* (PD-1)
243 gene expression; expression score for reported gene signatures related to T cells, immune
244 cells (non-T cells), and stromal cells and their products; T cell to stroma enrichment (TSE)
245 score; categories of the TSE score (negative, neutral or positive); and T cell receptor (TCR)
246 diversity index estimated with tcR v2.3.2[33].
247

248 It is noteworthy that patients with a positive TSE score were enriched for biopsies from
249 lymph nodes (Fisher's exact test $p < 0.001$), whereas patients with a neutral TSE score
250 were enriched for females (Fisher's exact test $p = 0.004$). The vast majority of tumors
251 with a negative TSE score (92%) were classified as stroma-rich or basal/squamous
252 according to transcriptomic subtypes of mUC[30]. TMB and APOBEC mutagenesis were
253 not different between the three TSE score groups (**Fig. 4**). Likewise, the distribution of
254 driver gene alterations, hotspot mutations and gene fusions were similar across TSE
255 score groups (**Supplementary Fig. 5**). Also, PD-L1 CPS was similar across the TSE
256 score groups (**Fig. 4**), whereas *CD274* (PD-L1) and *PDCD1* (PD-1) gene expressions
257 were higher for patients with a positive *vs* negative TSE score (**Supplementary Fig.**
258 **6**). When assessing the relative abundance of immune cell populations, we observed
259 that the fraction of myeloid dendritic cells was high in patients with a positive TSE score
260 (**Supplementary Fig. 7-8**). Furthermore, the TCR diversity was higher and the number

261 of hyperexpanded clones was lower in patients with a positive *vs* negative TSE score
262 (**Fig. 4, Supplementary Fig. 7, Supplementary Fig. 9**).
263

264 **The TSE score is a superior predictor for response and survival compared to**
265 **genomic metrics**

266 To evaluate the TSE score, TMB, APOBEC mutagenesis and their combinations as
267 predictors of response to pembrolizumab, ROC curves were analyzed (**Fig. 5a**). The
268 TSE score was superior to TMB and APOBEC mutagenesis to identify responders from
269 non-responders (**Fig. 5a**; DeLong's test $p = 0.006$ and $p = 0.003$ for AUC of TSE score
270 *vs* TMB and APOBEC mutagenesis, respectively). The AUC of the TSE score did not
271 improve when combined with TMB and/or APOBEC mutagenesis. Furthermore,
272 patients with a positive TSE score had a longer overall survival (OS) and progression-
273 free survival (PFS) when compared to other patients (**Fig. 5b)**. Multivariate cox
274 regression analysis, using continuous values, showed that the TSE score had a
275 superior predictive value for OS (TSE score $p < 0.001$; TMB $p = 0.21$; APOBEC $p =$
276 0.25) and PFS (TSE score $p = 0.002$; TMB $p = 0.32$; APOBEC $p = 0.27$) than TMB and
277 APOBEC mutagenesis (**Fig. 5b-d)**.

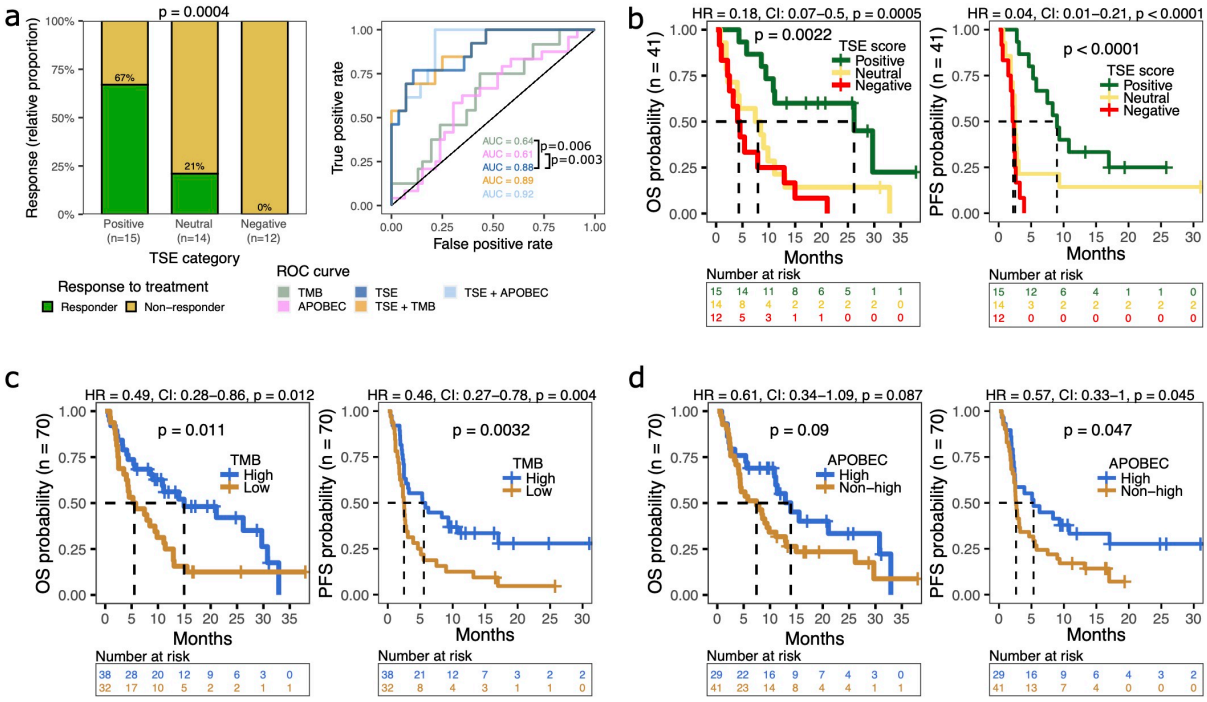

Fig. 5: Association of the TSE score, TMB and APOBEC mutagenesis with response to pembrolizumab and overall and progression-free survival.

(a) Bar graphs display the relative proportion of responders and non-responders in patients with a positive, neutral, or negative TSE score. P-value of TSE score positive *vs* negative was determined using the Fisher's exact test. Receiver operating characteristic (ROC) curves of TSE score, TMB, APOBEC mutagenesis (enrichment for APOBEC-associated mutations), and their combinations were constructed using continuous variables. The area under the curve (AUC) is displayed per condition, and p-values reflect DeLong's test of AUC's. (**b)** Overall survival (OS) and progression-free survival (PFS) probability in patients with a positive, neutral or negative TSE score (n = 41); **(c)** in patients with high or low TMB (n = 70); and (**d)** in patients with high or non-high APOBEC mutagenesis (n = 70). Log-rank test was applied to survival curves. For TSE score, hazard ratio (HR) was calculated for positive *vs* negative. CI = confidence interval.

294 **The TSE score as a predictor for response to pembrolizumab was validated in**
295 **independent cohorts of patients with urothelial cancer**

296 The predictive value of the TSE score for response to ICIs was validated in two
297 independent cohorts of UC patients from the IMvigor210[20] (n = 348) and ABACUS[18] (n
298 = 84) trials. First, the IMvigor210 trial evaluated the efficacy of atezolizumab (anti-PD-
299 L1) in patients with platinum-refractory locally advanced or mUC. The TSE score was
300 predictive for response (based on best overall response according to RECIST v1.1) to
301 anti-PD-L1 in this cohort. It is noteworthy that the AUC of the TSE score (AUC = 0.65)
302 was similar to the AUC of TMB (AUC = 0.71). Patients with a positive TSE score had
303 a higher response rate (36%) than patients with a neutral (18%) or negative (13%) TSE
304 score. A longer OS was observed in patients with a positive TSE score than other
305 patients ($p < 0.001$) (**Fig. 6a**). In the second validation cohort from the ABACUS trial,
306 the TSE score was also predictive for response (defined as a pathological complete
307 response (pCR) at cystectomy) to neoadjuvant treatment with atezolizumab in patients
308 with MIBC. In this cohort, TMB failed to predict response to neoadjuvant treatment[18],
309 and the AUC for the TSE score (AUC = 0.74) was higher than the AUC of TMB (AUC
310 = 0.51). The pCR rate was 44% for patients with a positive TSE score and was higher
311 compared to patients with a negative TSE score (9%, $p = 0.009$). In addition, patients
312 with a positive TSE score experienced a longer recurrence-free survival (**Fig. 6b**).
313 Together, these results suggest that contrary to TMB or ABOPEC mutagenesis, the
314 TSE score is a robust marker that predicts response to anti-PD-1 as well as anti-PD-
315 L1 in both metastatic and primary UC.

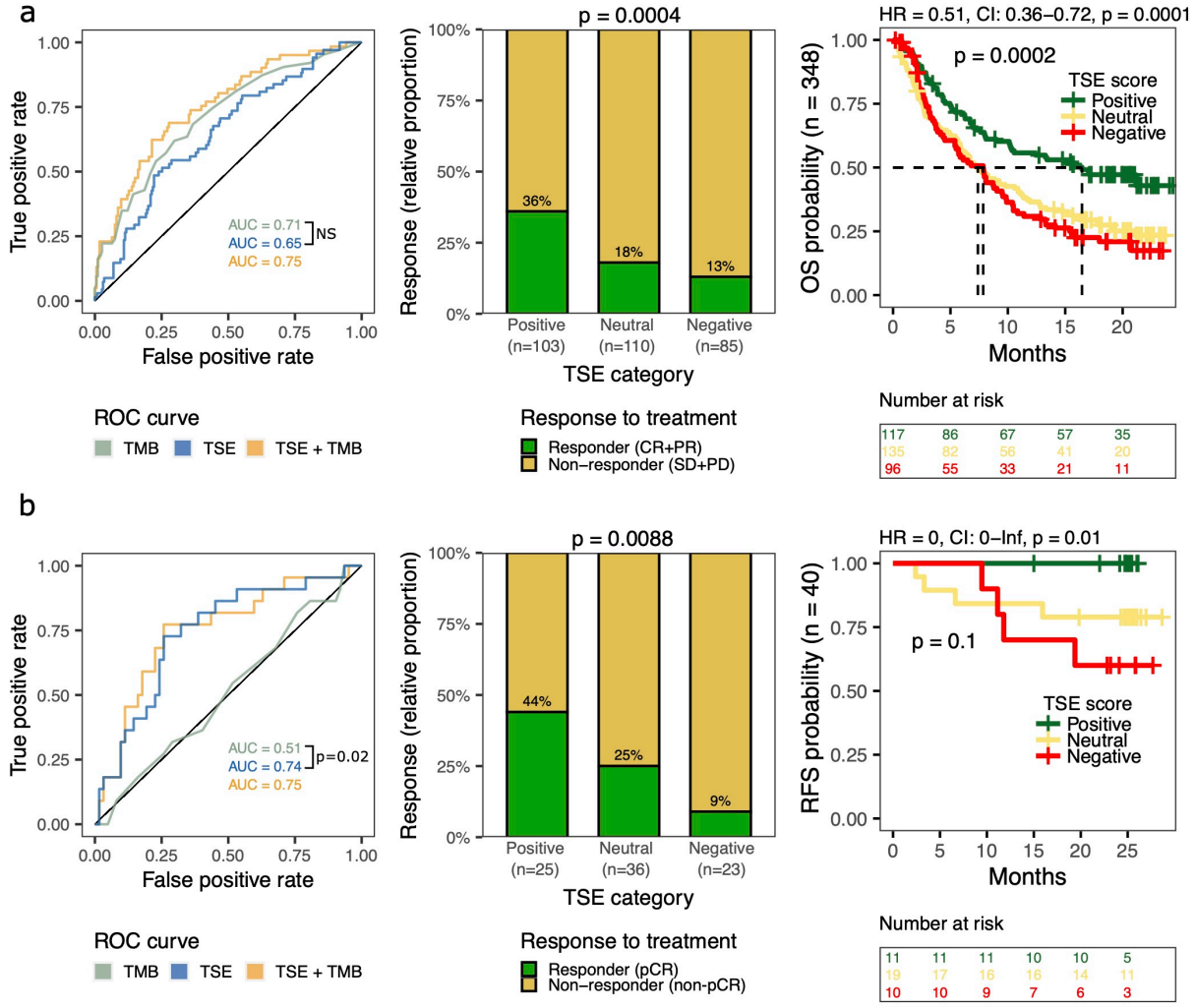

Fig. 6: Predictive value of the TSE score for response to ICIs in two independent cohorts of patients with urothelial carcinoma.

Validation of the T cell-to-stroma enrichment (TSE) score in the **(a)** IMvigor210 cohort (n = 348) and the **(b)** ABACUS trial (n = 84). *Left graphs:* Receiver operating characteristic curves of the TSE score, tumor mutational burden (TMB) and their combination. P-values reflect DeLong's test of AUC generated for the TSE score *vs* TMB (NS = not significant). *Middle graphs:* The bar graphs display the relative proportion of responders and non-responders in patients with a positive, neutral, or negative TSE score. In the IMvigor210 cohort (n = 298 response to treatment available), responders were defined as those patients with a complete response (CR) or partial response (PR), and non-responders as those with stable disease (SD) or progressive disease (PD) as best overall response according to RECIST v1.1. In the ABACUS trial, responders were patients with a pathological complete response (pCR) at

329 cystectomy. Fisher's exact test was applied on the proportion of responders in patients with a
330 positive *vs* negative TSE score. *Right graphs:* Overall survival (OS) probability was available
331 for all patients in the IMvigor210 cohort and recurrence-free survival (RFS) was available for
332 40 patients in the ABACUS cohort. Log-rank test was applied to survival curves. Hazard ratios
333 (HR) were calculated for patients with a positive *vs* negative TSE score. CI = confidence
334 interval.
335
336

337 **Discussion**

338 In this study, we aimed to identify a marker that predicts response to pembrolizumab
339 by analyzing the genomic and transcriptomic profiles of metastatic lesions from
340 patients with mUC prior to treatment. We observed that gene expression signatures of
341 T cells or stromal cells and their products associated with either response or resistance
342 to pembrolizumab. We translated these findings into the TSE score, a single metric
343 that reflects the abundance of T cells relative to that of stromal cells and their products.
344 This TSE score acted as a predictor for response and correlated with survival in our
345 patient cohort. The predictive value of the TSE score was validated using two
346 independent cohorts of patients with primary and metastatic urothelial cancer treated
347 with atezolizumab.

348 In line with previous studies in patients with mUC[13,16,25,26], high TMB and high APOBEC
349 mutagenesis were associated with response to pembrolizumab in our cohort. However,
350 the predictive value of both genomic scores was limited since approximately 20% of
351 patients with low TMB or non-high APOBEC mutagenesis still had benefit from
352 treatment. PD-L1 CPS failed to predict outcome in our cohort. The TSE score, derived
353 from transcriptomics related to T cells and stromal cells and their products, resulted in
354 a better predictive value when compared to TMB, APOBEC or single gene signatures.
355 In fact, the large majority of patients with a positive TSE score responded to
356 pembrolizumab and patients had superior OS and PFS when compared to other
357 patients. In contrast, none of the patients with a negative TSE score had a response
358 to treatment. At transcriptomic level, tumors of these patients were characterized by
359 signatures related to TGF-β signaling and epithelial-to-mesenchymal transition (EMT),
360 most of these tumors were of the stroma-rich or basal-squamous mUC subtype.
361 Potentially, a negative TSE score reflects an immune-evasive mechanism limiting T

362 cell influx and migration caused by an overly active stromal compartment. Indeed,
363 TGF-β signaling has previously been associated with an immune excluded phenotype,
364 and a fibroblast and collagen-rich tumor stroma in anti-PD-L1 resistant mUC[20]. In
365 addition, in patients with mUC treated with anti-PD-1, EMT-like gene expression by
366 stromal cells was related to treatment resistance, even in the presence of T cell
367 infiltration[34]. The association between a fibrotic subtype of the tumor micro-
368 environment and both non-response and poor survival has been observed in patients
369 with mUC and other cancers[21].

370 The predictive value of the TSE score has been validated in two independent patient
371 cohorts, namely patients with mUC treated with atezolizumab (IMvigor210 trial) and
372 patients with MIBC treated with neo-adjuvant atezolizumab (ABACUS trial). The TSE
373 score was able to predict response to atezolizumab in both cohorts, and was
374 associated with improved OS in the IMvigor210 cohort, although its predictive value
375 appeared less strong compared to our cohort. Possibly this can be explained by
376 differences with respect to timing of tumor tissue collection relative to treatment
377 initiation (immediately prior *vs* <2 years prior to treatment). In the ABACUS cohort, and
378 in line with the current cohort, tissue samples were obtained directly prior to therapy
379 initiation and may therefore better reflect the transcriptomic state of the tumor,
380 suggesting that fresh biopsies may improve the predictive power of the TSE score.
381 Importantly, based on the findings from the ABACUS cohort, the TSE score seems to
382 be applicable beyond the metastatic setting, confirming the robustness of the TSE
383 score as a predictor for response to ICIs in patients with urothelial cancer.

384 A limitation of this study is the relatively small cohort size, which reduced our statistical
385 power to further improve the stratification of patients within the TSE score groups. More
386 specifically, the group of patients with a neutral TSE score showed a response rate of

387 approximately 20% in all three independent cohorts. Identifying responders within this
388 group using genomics, transcriptomics and other molecular markers, would be
389 necessary to improve the selection of these patients for ICIs.

390 In conclusion, analysis of the transcriptome identified the TSE score as a clinically
391 relevant marker to select patients with UC for PD-(L)1-targeting ICIs, both in the
392 primary and metastatic setting. Since a negative TSE score identifies patients who will
393 not derive benefit from treatment with PD-(L)1-targeting ICIs, future studies are
394 warranted to adapt treatment for these patients in order to improve outcomes.

395

396

397 **Methods**

398 **Patient cohort and study design**

399 Between March 1st 2013 and March 31st 2020, patients with advanced or mUC from
400 31 Dutch hospitals were included in the nationwide Center for Personalized Cancer
401 Treatment (CPCT-02) biopsy protocol (NCT01855477). The study protocol was
402 approved by the medical ethics review board of the University Medical Center Utrecht,
403 the Netherlands. Written informed consent was obtained from all participants prior to
404 inclusion in the trial. The study population consisted of 288 patients who were
405 scheduled for 1st or 2nd line palliative systemic treatment. Fresh-frozen metastatic
406 tumor biopsies and matched normal blood samples were collected from 256 patients
407 as described previously[29]. WGS was successfully performed for 184 patients. Seventy
408 patients started a new line of pembrolizumab monotherapy and were included in the
409 current analysis. Matched RNA-seq was available for 41 patients. WGS, RNA-seq and
410 clinical data are available through the Hartwig Medical Foundation at
411 https://www.hartwigmedicalfoundation.nl, under request number DR-176.

412 A summary of all genomic and transcriptomic results as well as clinical data and
413 response to treatment are available in **Supplementary Table 4**.

414

415 **Treatment and assessment of response**

416 Patients were treated with pembrolizumab, 200 mg intravenously every three weeks,
417 or 400 mg every six weeks. Tumor response evaluation was performed using
418 computed tomography every 12 weeks. Treatment response was measured according
419 to response evaluation criteria in solid tumors (RECIST) v1.1. Data cut-off was set at
420 July 1st, 2020, resulting in a minimal follow-up of 6 months for all patients with a
421 response to treatment. Response was assessed at six months of therapy and patients

422 were classified as responder when they showed ongoing complete or partial response,
423 or stable disease. Patients were classified as non-responder when they had
424 progressive disease within six months after treatment initiation. Patients treated
425 beyond initial radiological disease progression were classified according to the date of
426 their first radiological progression event.
427

428 **PD-L1 immunohistochemistry and scoring**

429 PD-L1 expression was assessed on metastatic tumor biopsies (paraffin embedded)
430 that were freshly obtained prior to start of pembrolizumab (n = 32) using the companion
431 diagnostic assay of pembrolizumab (PD-L1 IHC 22C3 pharmDx, Agilent Technologies,
432 Carpinteria, CA, USA). When no fresh tumor biopsy was available, archival tumor
433 tissue (primary tumor or metastasis) was used (n = 8). All tissues were assessed for
434 the PD-L1 combined positivity score (CPS) by an expert genitourinary pathologist
435

436 **Whole-genome sequencing and analysis**

437 Alignment and pre-processing of WGS data, and subsequent detection of driver genes,
438 mutational signatures, genomic subtypes, homologous recombination (HR) deficiency,
439 structural variants, chromothripsis events and apolipoprotein B mRNA-editing enzyme,
440 catalytic polypeptide-like (APOBEC) mutagenesis have been previously
441 described[29,30,35]. APOBEC enriched tumors were classified as high when enrichment
442 (E) for APOBEC-related mutations was $E \geq 3$, medium when $2 \leq E < 3$ and low when
443 $E < 2$. The transcriptomic subtype of each sample was identified when the mean
444 (normalized) expression of all genes associated with a specific subtype[30] was the
445 highest across all subtypes. The clonal fraction of mutations was estimated as

446 previously described[36]. In this study, mutations were considered clonal when the
447 variant copy number was >0.75.

448

449 **RNA-sequencing**

450 Alignment and pre-processing of RNA-seq data, transcript normalization, and
451 subsequent analysis of pathway activity, and immune cell abundance have been
452 previously described[30].

453

454 **Gene signatures and the T cell-to-stroma enrichment score**

455 A list of 37 gene signatures representing immune and stromal cells and their products
456 was built from previously published resources (**Supplementary Table 2 and**
457 **Supplementary Table 5**). Normalized gene expression levels were median centered,
458 and the signature score was calculated as the mean expression of all genes per
459 signature.

460 Hierarchical clustering of gene signatures (**Fig. 4**) showed that cluster one, enriched
461 for responders, had a high signature score for immune cells and a low signature score
462 for stromal cells. On the contrary, cluster three with only non-responders, had a low
463 signature score for immune cells and a high signature score for stromal cells. This
464 result suggested that gene signatures representing immune cells may predict response
465 to pembrolizumab, while gene signatures for stromal cells may predict non-response
466 to pembrolizumab. However, the contribution of each gene signature to the cluster of
467 patients identified may vary. Thus, gene signatures with high standard deviation were
468 considered to have a high discriminatory power. We also observed that all signatures
469 were highly correlated within the group of immune cells and stromal cells. Applying
470 hierarchical clustering, we identified a group of T cell (Cytotoxic CD8 T cell, T cell

471 inflamed GEP, tGE8, T cell signature, IFN gamma, Immune gene signature and
472 chemoattractants) and stromal cell (Stromal signature, Fibroblasts, EMT/stroma core
473 genes, CAF, TBRS) signatures with a similar transcriptomic profile (**Supplementary**
474 **Fig. 4**). These signatures also had a high discriminatory power and high predictive
475 value as shown by the AUC of ROC curves for response to pembrolizumab
476 (**Supplementary Table 3**). To compare the contribution of both groups of signatures,
477 the mean of the selected signature scores for T cells and stromal cells was calculated.
478 These two metrics were considered to represent the global T cell and global stromal
479 cell signatures. Combining several signature scores into one global gene signature
480 also filters out the noise that individual signatures may have. According to multivariate
481 logistic regression analysis, the global signature scores for T cells and stromal cells
482 had independent predictive power for responders (Coefficient = 3.03, $p = 0.005$) and
483 non-responders (Coefficient = -2.40, $p = 0.010$), respectively. However, the arithmetic
484 difference of these global signatures (T cells minus stromal cells) showed a better
485 predictive value than the global signatures separately or single gene signatures
486 (**Supplementary Table 3**). This metric was named the T cell-to-stroma enrichment
487 (TSE) score because a positive TSE score points to an enrichment for T cells, while a
488 negative TSE score ($\leq$-0.5) points to an enrichment for stromal cells and their products.
489 The TSE score can also be interpreted as a ratio between T cell and stromal cell
490 signatures because the normalized gene expression data are raw counts transformed
491 on the log2 scale[1].

492 Given the high concordance between the TSE score and the three clusters of patients
493 from **Fig. 4**, patients were stratified into three groups according to their TSE score. The
494 TSE score = 0.5 was selected as cut-off because the three groups of patients obtained
495 resembled the original clusters from **Fig. 4**. Thus, patients with a TSE score $\geq$ 0.5 were

496 considered to have a positive TSE score, patients with a TSE score ≤ -0.5 were
497 considered to have a negative TSE score and other patients were considered to have
498 a neutral TSE score.

499

500 **TCR repertoire**

501 RNA-seq data was processed with MiXCR v3.0.13[37] to estimate the TCR repertoire
502 diversity. Samples with >100 total TCR reads were considered for downstream
503 analysis. The relative proportion (*R*) was used to group clonotypes as hyperexpanded
504 when *R* > 10%, large when *R* = 1%-10%, small when *R* represented more than one
505 clonotype but R < 1%, and rare when only one read supported a clonotype.

506

507 **Statistical analysis**

508 Analyses were performed using the statistical analysis platform R v4.1.0[38]. Fisher's
509 exact and Wilcoxon-rank sum tests were used for comparison between groups.
510 DeLong's and log-rank tests were used for comparing receiver operating
511 characteristics (ROC) and Kaplan-Meier survival curves, respectively. For multivariate
512 analyses, the Cox proportional hazards regression analysis and the t-statistic for
513 logistic regression analysis were applied.

514

515 **Data availability**

516 WGS, RNA-seq and clinical data are available through the Hartwig Medical Foundation
517 at https://www.hartwigmedicalfoundation.nl, under request number DR-176. The script
518 to calculate the TSE score from RNA normalized counts is available at
519 https://github.com/ANakauma/TSEscore_ICIs.

520

521 **Authors' disclosures of potential conflicts of interest**

522 Martijn P. J. Lolkema has received research support from JnJ, Sanofi, Astellas and
523 MSD, and consultancy fees from Incyte, Amgen, JnJ, Bayer, Servier, Roche, INCa,
524 Pfizer, Sanofi, Astellas, AstraZeneca, Merck Sharp & Dohme, Novartis, Julius Clinical
525 and the Hartwig Medical Foundation (all paid to the Erasmus MC Cancer Institute).

526 Debbie G.J. Robbrecht has received research support from Treatmeds and
527 consultancy fees from Bristol-Myers Squibb, Bayer, AstraZeneca, Merck, Pfizer (all
528 paid to the Erasmus MC Cancer Institute).

529 Ronald de Wit has received consultancy fees from Sanofi, Merck, Astellas, Bayer,
530 Hengrui and Orion, speaker fees from Sanofi and Astellas, research support from
531 Sanofi and Bayer (all paid to the Erasmus MC Cancer Institute).

532 Astrid A.M. van der Veldt has received consultancy fees from for BMS, MSD, Merck,
533 Novartis, Roche, Sanofi, Pierre Fabre, Ipsen, Eisai, Pfizer (all paid to the Erasmus MC
534 Cancer Institute).

535 Michiel S. van der Heijden has received research support from Bristol-Myers Squibb,
536 AstraZeneca and Roche, and consultancy fees from Bristol-Myers Squibb, Merck
537 Sharp & Dohme, Roche, AstraZeneca, Seattle Genetics and Janssen (all paid to the
538 Netherlands Cancer Institute).

539 Joost L. Boormans has received research support from Decipher Biosciences and
540 Merck Sharp & Dohme, and consultancy fees from Merck Sharp & Dohme, Eight
541 Medical, Ambu, APIM therapeutics, Bristol-Myers Squibb, Astellas Roche and Janssen
542 (all paid to the Erasmus MC Cancer Institute).

543 Niven Mehra has received research support from Astellas, Janssen, Pfizer, Roche and
544 Sanofi Genzyme, and consultancy fees from Roche, MSD, BMS, Bayer, Astellas and
545 Janssen (all paid to the Radboud University Medical Center).

Hans M. Westgeest has received consultancy fees from Roche and Astellas (all paid to the Amphia hospital, Breda), Paul Hamberg has received consultancy fees from Astellas, Merck Sharp & Dohme, Pfizer AstraZeneca, Bristol-Myers Squibb and Ipsen. Maureen J.B. Aarts has received advisory board / consultancy honoraria from Amgen, Bristol Myers Squibb, Novartis, MSD-Merck, Merck-Pfizer, Pierre Fabre, Sanofi, Astellas, Bayer, research grants from Merck-Pfizer, and not related to current work and paid to Maastricht UMC+ Comprehensive Cancer Center.

Geert J.L.H. van Leenders has received research grants from Roche and AstraZenaca, and has been member of advisory boards of Roche and Merck.

Maud Rijnders, J. Alberto Nakauma-González, Alberto Gil-Jimenez and Jens Voortman declare no competing interests.

References

1. Bellmunt J, de Wit R, Vaughn DJ, et al: Pembrolizumab as Second-Line Therapy for Advanced Urothelial Carcinoma. N Engl J Med 376:1015-1026, 2017
2. Rijnders M, de Wit R, Boormans JL, et al: Systematic Review of Immune Checkpoint Inhibition in Urological Cancers. Eur Urol 72:411-423, 2017
3. Fradet Y, Bellmunt J, Vaughn DJ, et al: Randomized phase III KEYNOTE-045 trial of pembrolizumab versus paclitaxel, docetaxel, or vinflunine in recurrent advanced urothelial cancer: results of > 2 years of follow-up. Ann Oncol, 2019
4. Balar AV, Castellano D, O'Donnell PH, et al: First-line pembrolizumab in cisplatin-ineligible patients with locally advanced and unresectable or metastatic urothelial cancer (KEYNOTE-052): a multicentre, single-arm, phase 2 study. Lancet Oncol 18:1483-1492, 2017
5. Balar AV, Galsky MD, Rosenberg JE, et al: Atezolizumab as first-line treatment in cisplatin-ineligible patients with locally advanced and metastatic urothelial carcinoma: a single-arm, multicentre, phase 2 trial. Lancet 389:67-76, 2017
6. Lee HH, Ham WS: Perioperative immunotherapy in muscle-invasive bladder cancer. Translational Cancer Research 9:6546-6553, 2020
7. Ghate K, Amir E, Kuksis M, et al: PD-L1 expression and clinical outcomes in patients with advanced urothelial carcinoma treated with checkpoint inhibitors: A meta-analysis. Cancer Treatment Reviews 76:51-56, 2019
8. Powles T, Csőszi T, Özgüroğlu M, et al: Pembrolizumab alone or combined with chemotherapy versus chemotherapy as first-line therapy for advanced urothelial carcinoma (KEYNOTE-361): a randomised, open-label, phase 3 trial. The Lancet Oncology 22:931-945, 2021
9. Galsky MD, Arija JÁA, Bamias A, et al: Atezolizumab with or without chemotherapy in metastatic urothelial cancer (IMvigor130): a multicentre, randomised, placebo-controlled phase 3 trial. The Lancet 395:1547-1557, 2020
10. Rijnders M, van der Veldt AAM, Zuiverloon TCM, et al: PD-L1 Antibody Comparison in Urothelial Carcinoma. Eur Urol 75:538-540, 2019
11. Powles T, Walker J, Andrew Williams J, et al: The evolving role of PD-L1 testing in patients with metastatic urothelial carcinoma. Cancer Treat Rev 82:101925, 2020
12. Cristescu R, Mogg R, Ayers M, et al: Pan-tumor genomic biomarkers for PD-1 checkpoint blockade-based immunotherapy. Science 362, 2018
13. Gupta S, Huang RSP, Stanke J, et al: Tumor mutational burden as a predictive biomarker for immune checkpoint inhibitor versus chemotherapy benefit in first-line metastatic urothelial carcinoma: A real-world study. Journal of Clinical Oncology 40:547-547, 2022
14. Marabelle A, Fakih M, Lopez J, et al: Association of tumour mutational burden with outcomes in patients with advanced solid tumours treated with pembrolizumab: prospective biomarker analysis of the multicohort, open-label, phase 2 KEYNOTE-158 study. Lancet Oncol 21:1353-1365, 2020
15. FDA Approves Pembrolizumab for Adults and Children With Tumor Mutational Burden–High Solid Tumors, 2020
16. Rosenberg JE, Hoffman-Censits J, Powles T, et al: Atezolizumab in patients with locally advanced and metastatic urothelial carcinoma who have progressed following treatment with platinum-based chemotherapy: a single-arm, multicentre, phase 2 trial. Lancet 387:1909-20, 2016
17. Tumeh PC, Harview CL, Yearley JH, et al: PD-1 blockade induces responses by inhibiting adaptive immune resistance. Nature 515:568-71, 2014
18. Powles T, Kockx M, Rodriguez-Vida A, et al: Clinical efficacy and biomarker analysis of neoadjuvant atezolizumab in operable urothelial carcinoma in the ABACUS trial. Nature Medicine 25:1706-1714, 2019
19. Sharma P, Retz M, Siefker-Radtke A, et al: Nivolumab in metastatic urothelial carcinoma after platinum therapy (CheckMate 275): a multicentre, single-arm, phase 2 trial. Lancet Oncol 18:312-322, 2017
20. Mariathasan S, Turley SJ, Nickles D, et al: TGFβ attenuates tumour response to PD-L1 blockade by contributing to exclusion of T cells. Nature 554:544-548, 2018
21. Bagaev A, Kotlov N, Nomie K, et al: Conserved pan-cancer microenvironment subtypes predict response to immunotherapy. Cancer Cell 39:845-865.e7, 2021
22. Teo MY, Seier K, Ostrovnaya I, et al: Alterations in DNA Damage Response and Repair Genes as Potential Marker of Clinical Benefit From PD-1/PD-L1 Blockade in Advanced Urothelial Cancers. Journal of Clinical Oncology 36:1685-1694, 2018
23. Mendelaar PAJ, Robbrecht DGJ, Rijnders M, et al: Genome-wide aneuploidy detected by mFast-SeqS in circulating cell-free DNA is associated with poor response to pembrolizumab in patients with advanced urothelial cancer. Molecular Oncology n/a, 2022
24. Vandekerkhove G, Lavoie J-M, Annala M, et al: Plasma ctDNA is a tumor tissue surrogate and enables clinical-genomic stratification of metastatic bladder cancer. Nature Communications 12:184, 2021
25. Snyder A, Nathanson T, Funt SA, et al: Contribution of systemic and somatic factors to clinical response and resistance to PD-L1 blockade in urothelial cancer: An exploratory multi-omic analysis. PLoS Med 14:e1002309, 2017

26. Galsky M, Saci A, Szabo PM, et al: Nivolumab in Patients with Advanced Platinum-Resistant Urothelial Carcinoma: Efficacy, Safety, and Biomarker Analyses with Extended Follow-up from CheckMate 275. Clin Cancer Res, 2020

27. Powles T, Sridhar SS, Loriot Y, et al: Avelumab maintenance in advanced urothelial carcinoma: biomarker analysis of the phase 3 JAVELIN Bladder 100 trial. Nature Medicine 27:2200-2211, 2021

28. Bellmunt J, de Wit R, Fradet Y, et al: Putative Biomarkers of Clinical Benefit With Pembrolizumab in Advanced Urothelial Cancer: Results from the KEYNOTE-045 and KEYNOTE-052 Landmark Trials. Clinical Cancer Research:OF1-OF11, 2022

29. Priestley P, Baber J, Lolkema MP, et al: Pan-cancer whole-genome analyses of metastatic solid tumours. Nature 575:210-216, 2019

30. Nakauma-González JA, Rijnders M, van Riet J, et al: Comprehensive Molecular Characterization Reveals Genomic and Transcriptomic Subtypes of Metastatic Urothelial Carcinoma. European Urology 81:331-336, 2022

31. Yu G, He QY: ReactomePA: An R/Bioconductor package for reactome pathway analysis and visualization. Molecular BioSystems 12:477-479, 2016

32. Wilkerson MD, Hayes DN: ConsensusClusterPlus: A class discovery tool with confidence assessments and item tracking. Bioinformatics 26:1572-1573, 2010

33. Nazarov VI, Pogorelyy VM, Komech EA, et al: tcR: An R package for T cell receptor repertoire advanced data analysis. BMC Bioinformatics 16:175, 2015

34. Wang L, Saci A, Szabo PM, et al: EMT- and stroma-related gene expression and resistance to PD-1 blockade in urothelial cancer. Nature Communications 9:3503, 2018

35. van Dessel LF, van Riet J, Smits M, et al: The genomic landscape of metastatic castration-resistant prostate cancers reveals multiple distinct genotypes with potential clinical impact. Nature Communications 10:1-13, 2019

36. Stephens PJ, Tarpey PS, Davies H, et al: The landscape of cancer genes and mutational processes in breast cancer. Nature 486:400-404, 2012

37. Bolotin DA, Poslavsky S, Mitrophanov I, et al: MiXCR: Software for comprehensive adaptive immunity profiling, Nature Publishing Group, 2015, pp 380-381

38. Team RC: R Core Team (2017). R: A language and environment for statistical computing. R Foundation for Statistical Computing, Vienna, Austria. URL http://www.R-project.org/.R Foundation for Statistical Computing-R Foundation for Statistical Computing, 2017